Effects of Crystallization Condition of Poly(butylene succinate) Component on the Crystallization of Poly(ethylene oxide) Component in Their Miscible Blends

Yong He,† Bo Zhu, Weihua Kai, and Yoshio Inoue*

Department of Biomolecular Engineering, Tokyo Institute of Technology, Nagatsuta 4259, Midori-ku, Yokohama 226-8501, Japan

Received March 17, 2004; Revised Manuscript Received August 12, 2004

ABSTRACT: The crystallization behavior of the poly(ethylene oxide) (PEO) component in poly(butylene succinate) (PBS)/PEO blends with the middle PEO content was investigated as a function of isothermal crystallization temperature of the PBS component ($T_{IC,PBS}$) using differential scanning calorimetry (DSC). It is found that the crystallization behavior of the PEO component in these blends is significantly affected by $T_{IC,PBS}$. Small-angle X-ray diffraction (SAXS) measurements were performed to explore the origin of the $T_{IC,PBS}$ dependence of crystallization of PEO component. On the basis of the SAXS measurements and the results of our previous work [*Macromolecules* **2004**, 37, 3337−3345], it is suggested that $T_{IC,PBS}$ controls the location distribution of the PEO component in the blends after the crystallization of the PBS component and thus significantly affects the crystallization behavior of PEO.

1. Introduction

So far, the confined and fractional crystallizations were found to occur in immiscible polymer blends,[1] microphase-separated block copolymers,[2] ultrathin films,[3] microdroplets,[4] and nanodroplets.[5] In our previous work, it was first reported that the confined and fractional crystallizations also occur in a miscible blend, such as the binary blend of poly(ethylene oxide) (PEO) and poly(butylene succinate) (PBS).[6]

Many works have addressed the crystallization and positional distribution in miscible blends containing a single crystallizable component.[7,8] However, few papers have investigated the microstructure of miscible blend containing two crystallizable components.[9] In this sense, the blends of PEO and PBS are of special interest as both component polymers are crystalline, and they are miscible in the melt state over the entire composition range.[6,10] In the previous paper, we have studied the miscibility, morphology, and crystallization behavior of the PEO/PBS blends using differential scanning calorimetry (DSC), high-resolution solid-state ^{13}C NMR spectroscopy, and wide- and small-angle X-ray diffraction.[6] The PEO and PBS are found to be miscible in the amorphous phase, and fractional crystallization is observed for the blends. The PEO component in the blend with PEO content less than 20 wt % is completely included and thus crystallizes in the region between PBS lamellae.

In the present paper, the crystallization behavior of the PEO component in the PBS/PEO blends will be further investigated. In the previous work, the crystallization behavior has been mainly studied for the blend with PEO content less than 20 wt %, where the PEO component crystallizes in the region between PBS lamellae.[6] This paper focuses on a new finding; that is, the crystallization of the PEO component in the PBS/PEO blends with middle content of PEO is greatly affected by the crystallization condition of PBS component when the blend is cooled from the melt.

In this paper, the crystallization and melting behavior of the PEO component in these blends are first investigated as a function of crystallization condition of the PBS component by DSC. Then, X-ray measurements were performed to try to shed light on the origin of the interesting crystallization phenomenon.

2. Experimental Section

2.1. Materials and Blend Preparation. Poly(ethylene oxide) with a number-average molecular weight $\boldsymbol{M}_n$ of 2.0×10^4 was purchased from Nacalai Tesque Inc. Japan. Poly(butylene succinate) ($\boldsymbol{M}_n = 2.2 \times 10^4$, $\boldsymbol{M}_w/\boldsymbol{M}_n = 2.1$) was kindly supplied by Showa Highpolymer Co. Japan. Before use, PEO and PBS were purified by precipitation respectively into *n*-hexane and ethanol from chloroform solutions. The melting points of pure PEO and PBS measured by DSC are 65 and 114 °C, respectively. The melt-crystallization temperatures are 40 and 77 °C, respectively, when they are cooled from the melt of 150 °C with a cooling rate of 10 °C/min.

Blends of PBS and PEO were prepared by solution casting with chloroform as a common solvent. Both polymers were dissolved and mixed in chloroform with the desired mass proportions (total polymer concentration was 2 wt %), well-stirred, and subsequently cast onto the Teflon dishes. The solvent was allowed to evaporate for 24 h, and the resulting films were further dried under vacuum at room temperature for 1 week. The cast films were subsequently compression molded between two Teflon sheets with an appropriate spacer for 2 min at 150 °C under a pressure of 5 MPa, using a laboratory press (MINI TEST PRESS-10, Toyoseiki Co., Japan).

After the compression, the sample is cooled fast to room temperature between two iron plates or transferred to an oven to allow the isothermal crystallization of the PBS component at a given temperature. The blends are denoted as *x*/*y*, where *x* and *y* are the weight percentages of PBS and PEO, respectively. For the blend *x*/*y* directly cooled to room temperature, it is coded as *x*/*y*RT. For that isothermally crystallized at a given temperature, it is coded as *x*/*y*IC*z*, where *z* is a two-digital number indicating the isothermal crystallization temperature. After crystallization, the sample was quenched into liquid nitrogen, and this sample is denoted as *x*/*y*ICzQ. After quenching, the sample was heated again to 75 °C to melt the PEO crystal, and the sample is then coded as *x*/*y*ICzQH.

2.2. Experimental Techniques. Differential scanning calorimetry (DSC) runs were performed on a Pyris Diamond

* Corresponding author: Tel +81-45-924-5794, Fax +81-45-924-5827, e-mail yinoue@bio.titech.ac.jp.

† Current address: Toray Fibers & Textiles Research Laboratories (China) Co., Ltd. (TFRC), 10th Floor, HSBC TOWER, 101 Yin Cheng East Road, Pudong New Area, Shanghai 200120, China.

10.1021/ma049482f CCC: $27.50
Published on Web 09/23/2004

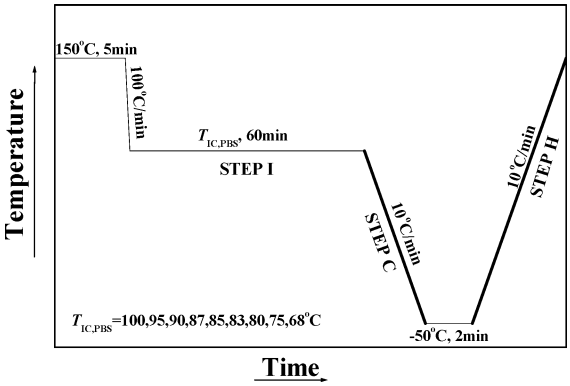

Figure 1. Thermal program used in this study to measure the crystallization and melting temperature of the PEO component as a function of the isothermal crystallization temperature $T_{IC,PBS}$ of the PBS component.

DSC (Perkin-Elmer Japan Co., Tokyo, Japan) under ultrapure nitrogen purge with 5.5−6.0 mg samples encapsulated in aluminum DSC pans. Before the DSC measurement, the calibration was always carried out with indium at the same scanning rate as employed in the measurements. A baseline was regularly checked for empty sample pan. The area and maximum of the crystallization exothermic peak and the melting endothermic peak were taken as the crystallization enthalpy and temperature (ΔH_c and T_c) and heat of fusion and temperature (ΔH_f and T_m), respectively. The mass crystallinity X_c was estimated from the ΔH_f value, assuming the heat of fusion $\Delta H_f°$ of 100 wt % crystalline PBS and PEO are 102[6] and 208 J/g, respectively.[11−14]

Wide-angle X-ray diffraction (WAXD) and small-angle X-ray scattering (SAXS) measurements were performed on a RINT-2000 system (40 kV and 200 mA) (Rigaku Co., Japan) at room temperature. Nickel-filtered Cu Kα radiation ($\lambda = 0.154$ nm) was used. WAXD patterns were recorded in the 2θ range of 5−55° at a scan speed of 1.0°/min. SAXS profiles were recorded in the 2θ range of 0.1−2.5°. Each step increased 2θ by 0.004°, and X-ray was collected for 20 s at each step.

3. Results

3.1. Crystallization Behavior of PEO Component. The thermal program shown in Figure 1 was employed to measure the crystallization temperature of PEO component ($T_{C,PEO}$) during dynamic cooling as a function of the isothermal crystallization temperature of PBS component ($T_{IC,PBS}$). In this thermal program, the blend was first melted at 150 °C for 5 min to erase the thermal history, quenched to $T_{IC,PBS}$ ($T_{IC,PBS}$ = 100−68 °C), and held at $T_{IC,PBS}$ for 1 h to complete the crystallization of PBS component (step I), then the blend system was cooled from $T_{IC,PBS}$ to −50 °C at a scanning rate of 10 °C/min (step C) followed a holding at −50 °C for 2 min, and finally the sample was heated to 150 °C at a scanning rate of 10 °C/min (step H). The crystallization temperature of PEO component ($T_{C,PEO}$) was determined in step C of the thermal program.

The DSC cooling curves recorded at step C are summarized in Figure 2 for PBS/PEO 25/75, 60/40, and 80/20 (w/w) blends. As the crystallization of PBS component has finished in step I, all the exothermal peaks appeared in these curves correspond to the crystallization of the PEO component. For the PBS/PEO 80/20 (w/w) blend, the crystallization behavior of the PEO component hardly changes with the change of the isothermal crystallization temperature of the PBS component $T_{IC,PBS}$, and the crystallization temperature of the PEO component $T_{C,PEO}$ during dynamic cooling is always about −10 °C independent of $T_{IC,PBS}$ (Figures 2 and 3), as usually observed for general polymer blends. In the PBS/PEO 25/75 (w/w) blend, the change of crystallization behavior of the PEO component with $T_{IC,PBS}$ is not obvious if the PBS component isothermally crystallizes at $T_{IC,PBS}$ ranging from 68 to 90 °C. However, a second weak crystallization appears at about −7 °C besides the main crystallization peak at about 34 °C if $T_{IC,PBS}$ is higher than 90 °C (Figure 2).

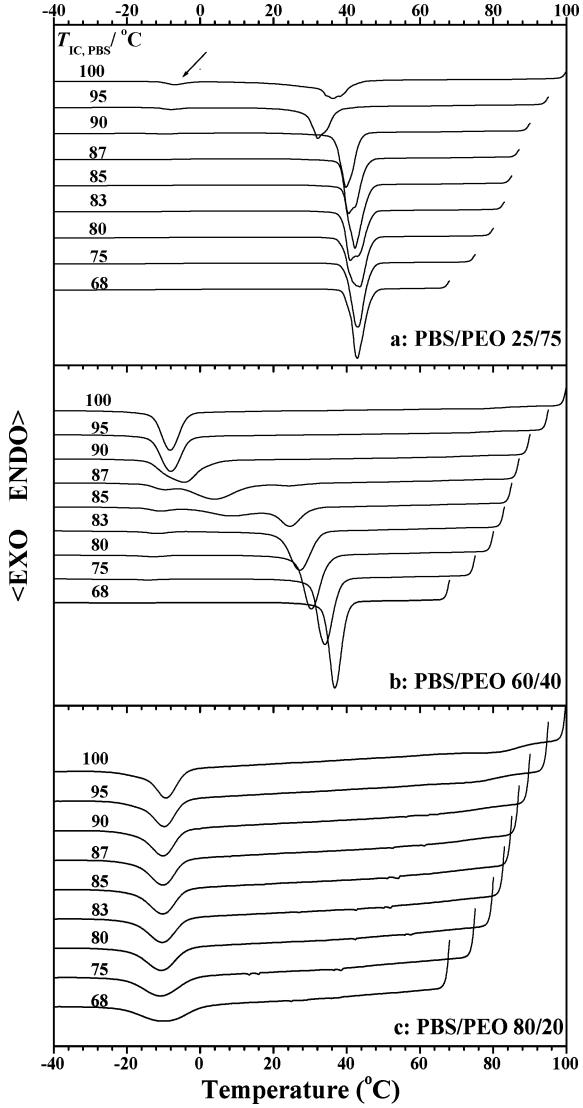

Figure 2. DSC cooling curves of (a) PBS/PEO 25/75, (b) 60/40, and (c) 80/20 (w/w) blends recorded at step C of the thermal program with a cooling rate of 10 °C/min.

For the PBS/PEO 60/40 (w/w) blend, the case is quite different from those of the 80/20 and 25/75 blends. A single crystallization peak is observed for the PEO component if the PBS component isothermally crystallizes at low and high $T_{IC,PBS}$s, while two or three crystallization peaks appear if the PBS component isothermally crystallizes at middle $T_{IC,PBS}$s (from ∼80 to ∼90 °C), where fractional crystallization occurs (Figure 2). Furthermore, a notable change of $T_{C,PEO}$ with $T_{IC,PBS}$ is observed; that is $T_{C,PEO}$ decreases with the increase of $T_{IC,PBS}$ (Figures 2 and 3).

The cases for the PBS/PEO 50/50 and 70/30 (w/w) blends are similar to that of the PBS/PEO 60/40 blend: for the PBS/PEO 50/50 blend two or three PEO crystallization peaks appear when $T_{IC,PBS}$ ranges from 90 to 83 °C, and for the 70/30 blend, the corresponding $T_{IC,PBS}$

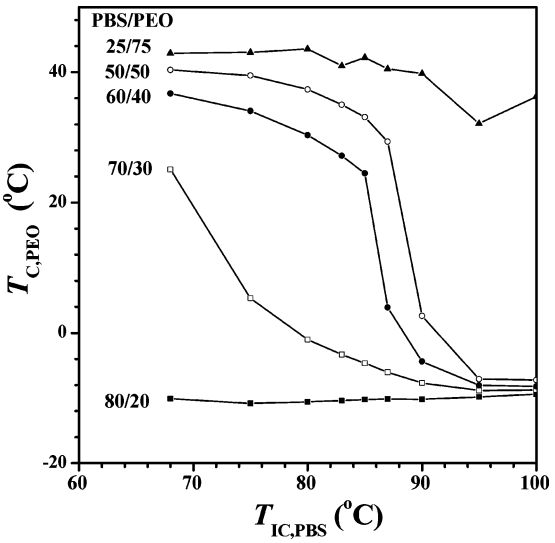

Figure 3. Crystallization temperature of the PEO component $T_{C,PEO}$ as a function of isothermal crystallization temperature $T_{IC,PBS}$ of the PBS component. $T_{C,PEO}$ was taken as the maximum of the crystallization peak or the main crystallization peak when two or more peaks were observed.

range is 83−68 °C; otherwise, a single crystallization is observed (the DSC curves of 50/50 and 70/30 blends are not shown here). Also, for both blends, $T_{C,PEO}$ decreases with the increase of $T_{IC,PBS}$ (Figure 3).

3.2. Melting Behavior of PEO Component. The DSC heating curves recorded at step H (see Figure 1 for thermal program) are plotted in Figure 4 for the PBS/PEO 25/75, 60/40, and 80/20 (w/w) blends as a function of $T_{IC,PBS}$. The melting behavior of the PEO component in the PBS/PEO 25/75 and 60/40 (w/w) blends is insensitive to the change of $T_{IC,PBS}$. However, the melting point of the PEO component in the PBS/PEO 80/20 blend increases with the increase of $T_{IC,PBS}$ besides the melting peak becomes sharper with the increase of $T_{IC,PBS}$ (Figure 4).

The melting point of the PEO component $T_{m,PEO}$ is plotted against $T_{IC,PBS}$ in Figure 5. $T_{m,PEO}$ of the PBS/PEO 25/75 (w/w) blend hardly changes with $T_{IC,PBS}$. $T_{m,PEO}$s of the 50/50 and 60/40 blends only show a decreasing tendency while those of the 70/30 and 80/20 blends show a significant increase with the increase of $T_{IC,PBS}$.

In general, the melting point of one polymer increases or at least does not change with the increase of its crystallization temperature. However, a very interesting behavior, that is, the melting point decreases with the increase of crystallization temperature, is observed for the blend system investigated here. $T_{m,PEO}$ is plotted against $T_{C,PEO}$ in Figure 6 for the PBS/PEO 70/30 blend. In this blend, $T_{m,PEO}$ does decrease with the increase of $T_{C,PEO}$.

3.3. Wide-Angle X-ray Diffraction (WAXD). The WAXD patterns of pure PBS, pure PEO, and their 60/40 blend measured at room temperature are shown in Figure 7. Before the measurement, the molded films of pure PBS and pure PEO were aged at room temperature for more than 10 days; 60/40IC75 and 60/40IC95 were the samples isothermally crystallized at 75 and 95 °C for 1 h, respectively; 60/40IC95Q was the sample quenched to liquid nitrogen after the isothermal crystallization at 95 °C; 60/40IC95QH was the sample reheated to 75 °C to melt the PEO crystals, which are formed during the quench. All blend films were kept at room

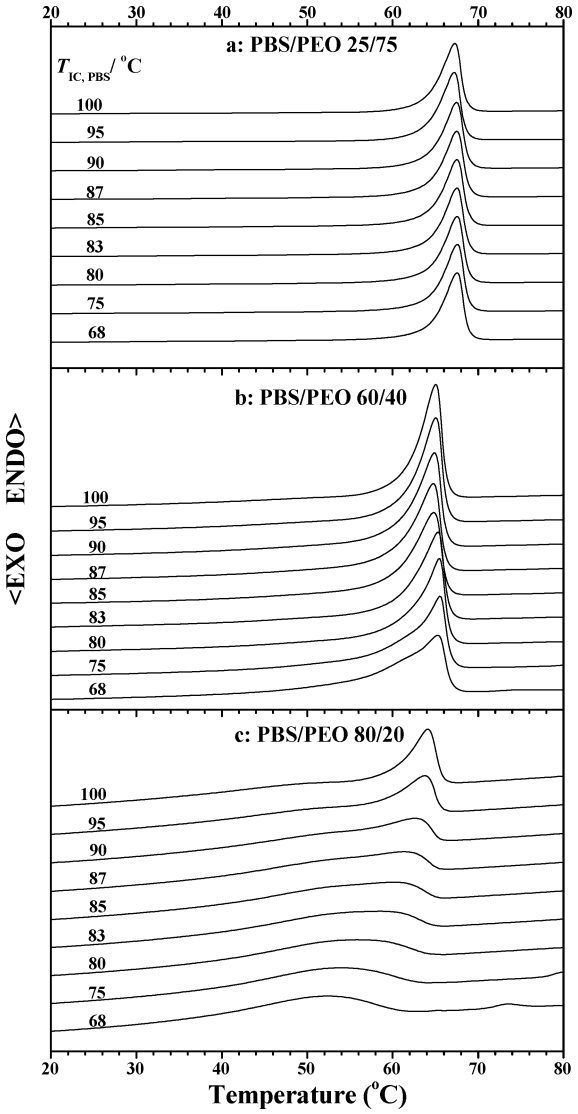

Figure 4. DSC heating curves of the PBS/PEO 25/75, 60/40, and 80/20 (w/w) blends. They are recorded at step H of the thermal program with a heating rate of 10 °C/min.

temperature in air after the thermal treatments. The patterns of both PEO and PBS crystals are clearly observed for the samples of 60/40IC75 and 60/40IC95Q. However, the diffraction peaks of PEO crystal cannot be detected for 60/40IC95 and 60/40IC95QH, indicating that the PEO component in these films is free from crystallization (this is also confirmed by DSC; the data are not shown). This result suggests that the PEO component in the 60/40 blend crystallizes only at a temperature lower than room temperature if the PBS component isothermally crystallizes at a temperature of 95 °C or higher than 95 °C, the same as in the 80/20 blend as revealed in the previous paper.[6]

3.4. Small-Angle X-ray Scattering (SAXS). The microstructures of the PBS/PEO blends were probed by SAXS at room temperature. The Lorentz-corrected SAXS profiles of the PBS/PEO 60/40 blend with different thermal histories are summarized in Figure 8, where the scattering vector $q = 4\pi \sin \theta/\lambda$ with 2θ as the scattering angle. The profile of pure PBS isothermally crystallized at 95 °C is also included in this figure as a reference. The position of the scattering peak from the blend shifts to a lower scattering angle with the increase of the isothermal crystallization temperature.

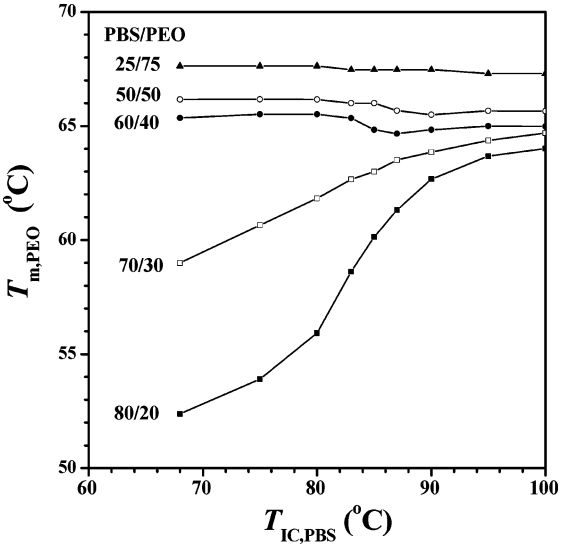

Figure 5. Melting temperature of the PEO component $T_{m,PEO}$ as a function of the isothermal crystallization temperature $T_{IC,PBS}$ of the PBS component.

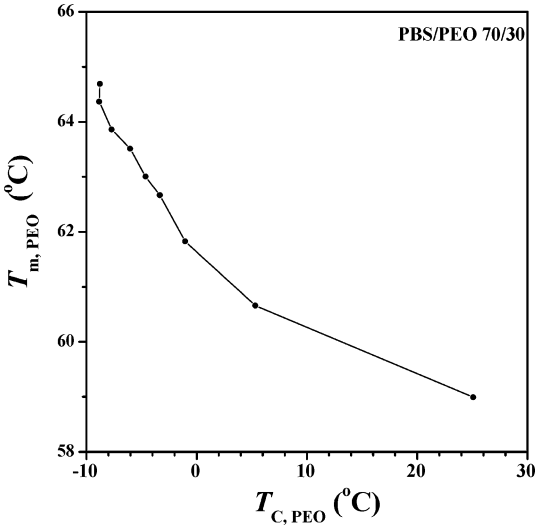

Figure 6. Plot of $T_{m,PEO}$ vs $T_{C,PEO}$ for the PBS/PEO 70/30 (w/w) blend.

For the 60/40IC95 films, the thermal treatment after the isothermal crystallization at 95 °C also significantly affects the profile. The scattering profile of 60/40IC95QH is almost the same as that of 60/40IC95 while the scattering peak of 60/40IC95Q shifts obviously to the high-q region.

The long period or the interlamellar spacing LP of PBS in the blend was calculated from the equation $LP = 2\pi/q^*$, where q^* is the peak value found in the Lorentz-corrected SAXS plot. The results are shown in Figure 9 and Table 1. For the samples isothermally crystallized at 95 °C, the long period LP increases with the increase of PEO content in the blend, W_{PEO}, in the investigated composition range. For the blends crystallized at 80 °C and room temperature, a maximum of LP is observed at W_{PEO} of about 30 and 40 wt %, respectively (Figure 9). From Table 1, it is clear that: (i) LP and Q_{exp} of 70/30 IC80Q are smaller than those of 70/30 IC80, respectively, and those of 60/40 IC95Q are smaller than those of 60/40 IC95, respectively, which indicate that LP and Q_{exp} decrease with the quench, that is, they decrease with the crystallization of the PEO component as the quench results in the crystallization

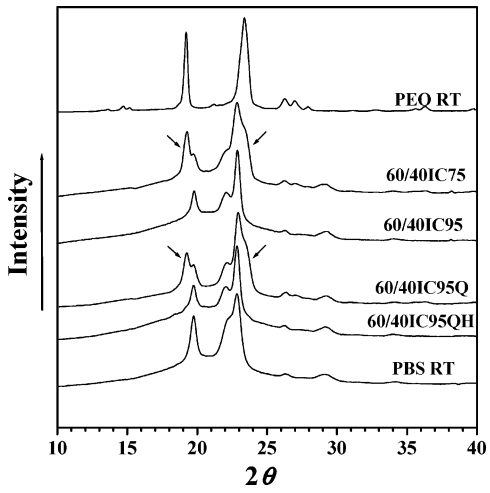

Figure 7. WAXD patterns of pure PBS, pure PEO and their 60/40 blend recorded at room temperature. Before the measurement, the molded films of pure PBS and pure PEO were aged at room temperature for at least 10 days. As to the films of the PBS/PEO 60/40 (w/w) blend, see sections 2.1 and 3.3 for the thermal history and the abbreviations. The arrow indicates the diffraction peak of PEO crystals.

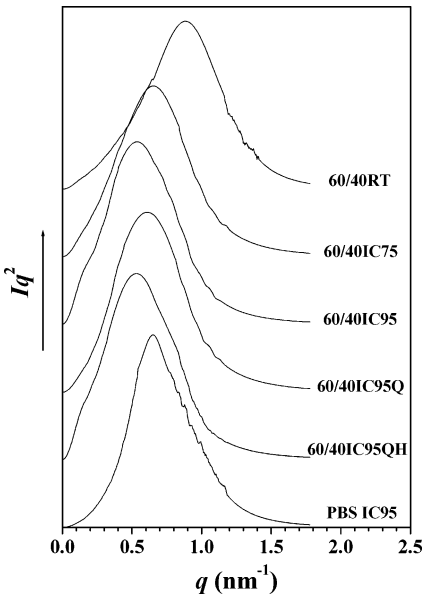

Figure 8. Lorentz-corrected SAXS profiles of the PBS/PEO 60/40 (w/w) blend. The curves were normalized and shifted vertically for clarity. See sections 2.1 and 3.3 for the thermal history and the abbreviation of the sample.

of PEO component. (ii) LP and Q_{exp} of 70/30 IC80QH are larger than those of 70/30 IC80Q and almost the same as those of 70/30 IC80, respectively. Similar results are also observed for PBS/PEO 60/40 blends. These suggest LP increases and returns to the original value once the PEO crystal is remelted during the following heating. These two points may imply that a cycle of crystallization and melt of PEO component does not affect the positional distribution of PEO component.

The SAXS invariant Q_{exp} is determined from the SAXS intensity profile and depicted in Figure 10. As the experimental invariant Q_{exp} is not on the absolute scale, in Figure 10 are only given the ratio of experimental invariants $Q_{exp,i}/Q_{exp,PBS}$ (experimental invariant of sample i/experimental invariant of pure PBS). $Q_{exp,i}/Q_{exp,PBS}$ is larger than 1 for all the investigated blends, indicating that the addition of PEO into the blend increases the invariant in this composition range.

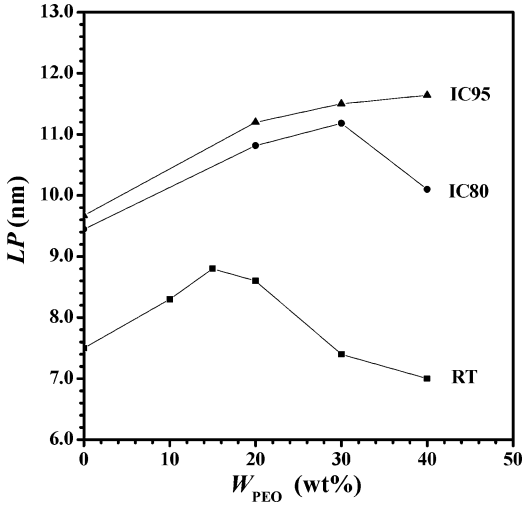

Figure 9. Relationship between the long period *LP* determined from Lorentz-corrected SAXS profile and the blend composition. IC95, IC80, and RT mean that the PBS component was crystallized at 95 °C, 85 °C, and room temperature, respectively, before the measurements.

Table 1. Long Periods *LP*s and Experimental Invariants Q_{exp}s of Pure PBS, PBS/PEO 70/30, and 60/40 Blends with Different Thermal Histories

sample[a]	q^*	*LP*/nm	Q_{exp}	sample[a]	q^*	*LP*/nm	Q_{exp}
PBS IC80	0.67	9.4	38	PBS IC95	0.65	9. 7	37
70/30 IC80	0.56	11.2	78	60/40 IC95	0.54	11.6	76
70/30 IC80Q	0.65	9.7	52	60/40 IC95Q	0.62	10.1	50
70/30 IC80QH	0.58	10. 9	80	60/40 IC95QH	0.53	11.7	74

[a] See sections 2.1 and 3.3 for the sample code and the thermal history.

In the case where the PEO component is completely in the amorphous state and is entirely incorporated in the amorphous layers between PBS lamellae, the invariant Q_{cal} of the ideal two phases can be calculated from the following equation:[15,16]

$$Q_{cal} = \phi(1-\phi)(\eta_c - \eta_a)^2 \quad (1)$$

Here ϕ is the volume crystallinity. η_c and η_a are the electron densities of 100% crystalline PBS and the amorphous phase in the blend, respectively. η_a is determined as

$$\eta_a = (\eta_{a,PEO}\phi_{a,PEO} + \eta_{a,PBS}\phi_{a,PBS})/(\phi_{a,PEO} + \phi_{a,PBS}) \quad (2)$$

where $\phi_{a,PEO}$ and $\phi_{a,PBS}$ are the volume fractions of PEO and amorphous PBS in the blend, respectively. The values of electron density of 100% crystalline PBS, 100% amorphous PBS, 100% crystalline PEO, and 100% amorphous PEO were calculated from their mass densities, namely, 0.716 ($\rho_{c,PBS}$ = 1.34 g/cm^3, refs 17, 18), 0.631 ($\rho_{a,PBS}$ = 1.18 g/cm^3, refs 19, 20), 0.676 ($\rho_{c,PEO}$ = 1.239 g/cm^3, refs 21, 22), and 0.612 ($\rho_{a,PEO}$ = 1.124 g/cm^3, refs 21, 22) mol of electrons/cm^3, respectively. ϕ, $\phi_{a,PEO}$, and $\phi_{a,PBS}$ can be estimated from the blend composition, mass crystallinity of the PBS component, and the densities.

In Figure 10 are shown the comparison of the ratio of experimental invariants ($Q_{exp,i}/Q_{exp,PBS}$, experimental invariant of sample *i*/experimental invariant of pure PBS) with the ratio of calculated ones ($Q_{cal,i}/Q_{cal,PBS}$). The $Q_{exp,i}/Q_{exp,PBS}$ value of 60/40RT and 60/40IC80 deviates

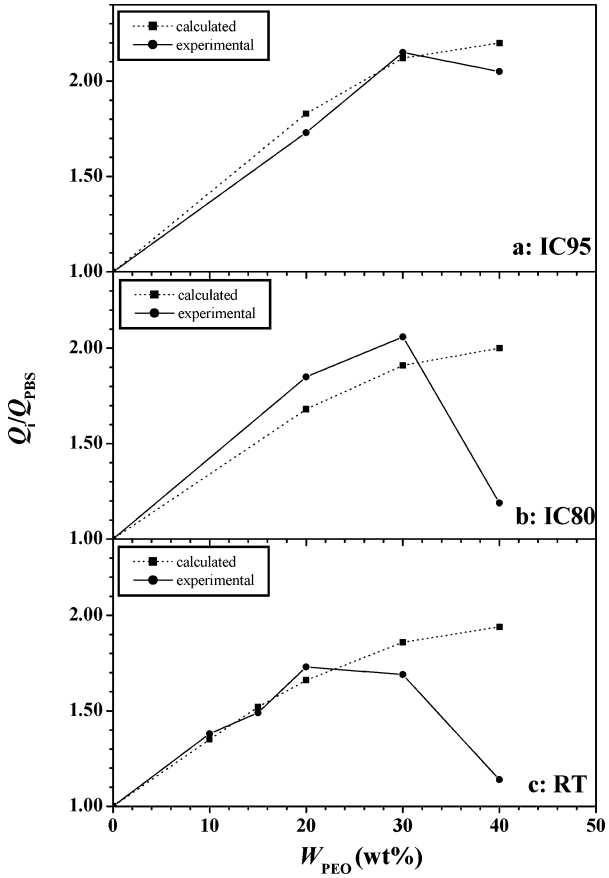

Figure 10. Ratios of the invariants *Q* of samples to that of pure PBS. IC95, IC80, and RT mean that the PBS component was crystallized at 95 °C, 85 °C, and room temperature, respectively, before the measurement.

from the corresponding $Q_{cal,i}/Q_{cal,PBS}$. This deviation should be due to (i) the crystallization of the PEO component and/or (ii) the exclusion of a part of the PEO component from the interlamellar region. However, the experimental ratios agree well with the calculated ones for the other samples, indicating that the PEO component is completely incorporated in the amorphous layers between the PBS lamellae in these samples.

4. Discussion

The DSC results have revealed that the isothermal crystallization temperature of the PBS component $T_{IC,PBS}$ significantly affects the crystallization and the melting behavior of the PEO component (Figures 2−5). The $T_{IC,PBS}$ dependence of the crystallization behavior of the PEO component in the blends with middle PEO contents is very similar to the composition dependence of crystallization of the PEO component as observed in the previous work.[6] Comparing Figure 2b of this article with Figure 2 of the previous work,[6] it is found that the DSC cooling curve changes with $T_{IC,PBS}$ in almost the same way as the changes of DSC curve with the blend composition. Including the $T_{C,PEO}-T_{IC,PBS}$ curves of the 60/40 and the 50/50 PBS/PEO blends and the $T_{C,PEO}-W_{PBS}$ curve into a single figure as shown in Figure 11, it is clear that the three curves can be superposed very well with each other with appropriate shifts; that is, the composition-temperature ($W_{PBS}-T_{IC,PBS}$) superposition is realized. In the previous work has been investigated the composition dependence of the crystallization of the PEO component, and it is revealed that the composition

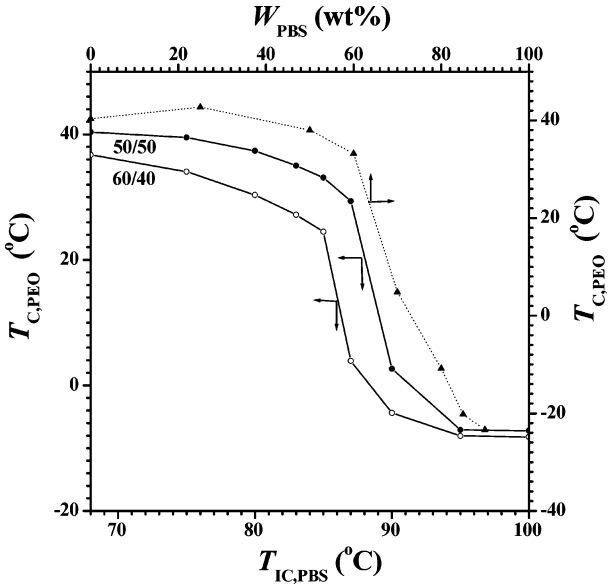

Figure 11. Composition−temperature superposition of $T_{C,PEO}$. The data of $T_{C,PEO}$ vs W_{PBS} were taken from our previous work.[6]

dependence mainly comes from the different distribution of the PEO component with the blend composition. In the PBS-rich blend, the PEO component is incorporated and crystallizes in between the PBS lamellae, and thus the crystallization temperature of PEO becomes very low. In the PEO-rich blend, the PEO component is mainly excluded from the interlamellar region of PBS. As a result, the PEO component in these blends crystallizes in low supercooling. Thus, the composition-temperature superposition may indicate that the $T_{IC,PBS}$ dependence of the crystallization of PEO component is in essence a reflection of that $T_{IC,PBS}$ effect on the distribution of positional location of PEO component. The $T_{IC,PBS}$ controls this positional distribution of the PEO component in the interlamellar, interfibrillar, and/or interspherulitic regions of the PBS component, and this distribution greatly influences the crystallization behavior of the PEO component.

One may wonder if different $T_{IC,PBS}$ results in different crystallinity of PBS and different composition of the amorphous PBS/PEO phase, which leads to the fractional crystallization behavior of PEO. In fact, $T_{IC,PBS}$ has few effects on the crystallinity of PBS under the studied condition. The crystallization enthalpy ΔH_c of the PBS component hardly changes with $T_{IC,PBS}$ under the studied conditions. The average ΔH_c for the nine $T_{IC,PBS}$s is 41.9 ± 0.6 J/g. ΔH_c for $T_{IC,PBS}$ = 100 °C is 42.5 J/g, for $T_{IC,PBS}$ = 80 °C is 41.9 J/g, and for $T_{IC,PBS}$ = 68 °C is 41.4 J/g. Correspondingly, the crystallinity of PBS component after the isocrystallization is 68 ± 1 wt % for average, 69 wt % for $T_{IC,PBS}$ = 100 °C, 68 wt % for $T_{IC,PBS}$ = 80 °C, and 67 wt % for $T_{IC,PBS}$ = 68 °C. Thus, the apparent concentration of the PEO component (before PEO crystallization) in the amorphous phase is 68.9 ± 0.7 wt % for average, 68.6 wt % corresponding to $T_{IC,PBS}$ of 100 °C, 68.9 wt % corresponding to $T_{IC,PBS}$ of 80 °C, and 67.3 wt % corresponding to $T_{IC,PBS}$ of 68 °C. Thus, in our opinion, $T_{IC,PBS}$ hardly changes the composition of the amorphous PBS/PEO phase after the crystallization of PBS component under the investigated conditions. Martuscelli et al. have studied the crystallization behavior of PEO component in its miscible blend with natural poly(3-hydroxybutyrate) (PHB) as a function of cooling rate.[23] The crystallization behavior of PEO component in PHB/PEO blend is similar to that observed in the present work. In their work, ΔH_c of PHB is quite different for different cooling rate, 70 J/g for cooling rate of 1 °C/min and 56 J/g for 20 °C/min. Thus, Martuscelli et al. suggested that (i) different ΔH_c of PHB lead to different consuming of heterogeneous nuclei and (ii) high ΔH_c of PHB means that few heterogeneous nuclei are left over to induce the crystallization of PEO component, and thus PEO molecules may crystallize only at high supercooling according to a homogeneous mode of nucleation.[23] Considering the ΔH_c of PBS hardly changes with $T_{IC,PBS}$, the interpretation of Martuscelli should be not appropriate for crystallization behavior of PEO observed in the present work.

The SAXS results have provided some evidences to support our suggestion. When the PBS component isothermally crystallizes at 95 °C, the long period *LP* increases with the increase of PEO content W_{PEO} up to W_{PEO} of 40 wt % (Figure 9). Also, $Q_{exp,i}/Q_{exp,PBS}$ agrees well with the corresponding $Q_{cal,i}/Q_{cal,PBS}$ within the experimental uncertainty (Figure 10a). These two facts indicate that the PEO component is incorporated in the interlamellar region of the PBS component under this condition. Furthermore, *LP* and the invariant decrease upon the crystallization of the PEO component during the quench while they return to the original values after melting PEO crystals in the following heating (Table 1), which should suggest the PEO component mainly crystallizes within the region between the PBS lamellae. On the basis of this analysis and combined the results of the previous work,[6] it is easy to understand that in the case of (high $T_{IC,PBS}$) the crystallization of the PEO component (in the blend with W_{PEO} of 40% or lower) is confined and only occurs at low temperature as the crystallization is mainly induced by less active heterogeneities of the nucleation at high supercooling or even homogeneous nucleation at extreme supercooling.

If the PBS component isothermally crystallizes at a temperature of 80 °C or lower, for the 60/40 blends, the long period *LP* drops and the $Q_{exp,i}/Q_{exp,PBS}$ value significantly deviates from the corresponding $Q_{cal,i}/Q_{cal,PBS}$ value (Figures 9 and 10). This result should come from the following two aspects: (i) the crystallization of the PEO component; (ii) exclusion of a part of the PEO component from the interlamellar region. The latter should be the main reason due to the drastic decrease of the invariant. The results of our previous work also support this point.[6] Thus, the PEO component is mainly distributed in the interfibrillar or interspherulitic region. In this case, the crystallization of the PEO component is mainly induced by active heterogeneities and processes at high temperature.

It is noteworthy that the referred suggestion of inclusion of PEO component into the interlamellar region at high $T_{IC,PBS}$ and the exclusion of a part of the PEO component from the interlamellar region at low $T_{IC,PBS}$ seems to contradict the common sense. Many reports suggested that the position distribution and segregation in crystalline blends during the crystallization of one component can be predicted from diffusion length δ:[24−26]

$$\delta = D/V \tag{3}$$

where *D* is the diffusivity of the noncrystallizable species in the blend and *V* is the velocity of the crystallization front. If the diffusion length δ is sufficiently small, the excluded component should reside in the interlamellar

region. Otherwise, it should locate between the fibrils and even between the spherulites. As the temperature, at which the maximum spherulite growth rate of the PBS is observed, is smaller than 60 °C,[27,28] the diffusion length δ should increase with the increase of $T_{IC,PBS}$ in the studied $T_{IC,PBS}$ range (68−100 °C). Thus, the position distribution of PEO component during the crystallization of PBS predicted from δ should be that lower $T_{IC,PBS}$ favors the inclusion of PEO component into the interlamellar region and higher $T_{IC,PBS}$ favors the exclusion of a part of the PEO component from the interlamellar region, which contradicts to our suggestion. Also, the present work is difficult to give a good interpretation to this contradiction and one may naturally doubt if our suggestion is true. However, the suggestion is partly supported by the SAXS analysis and can explain all the experimental results. In our opinion, no other hypothesis can give a better interpretation than it at the present stage. Anyway, further work is required to judge whether it is right.

For the PBS/PEO 80/20 blend, the long period *LP* is obviously larger than that of pure PBS, and the value of $Q_{exp,i}/Q_{exp,PBS}$ locates in the line of $Q_{cal,i}/Q_{cal,PBS}$ even when $T_{IC,PBS}$ is lower than 80 °C (Figures 9 and 10). This indicates that the PEO component in this blend is always incorporated in the interlamellar region independent of $T_{IC,PBS}$. Therefore, its crystallization occurs at low temperature regardless of $T_{IC,PBS}$, as shown in Figures 2 and 3.

On the other side, most of the PEO component in the 25/75 PBS/PEO blend is excluded from the interlamellar region for all $T_{IC,PBS}$. To some extent, it crystallizes in a similar way as the pure PEO, free from $T_{IC,PBS}$.

As the $T_{IC,PBS}$ dependence of the melting behavior of the PEO component (Figures 4 and 5), the mechanism is not clear in the present stage. One possible reason for the increasing of $T_{m,PEO}$ with $T_{IC,PBS}$ for the 80/20 and 70/30 PBS/PEO blends is that the thickness of the interlamellar phase of PBS increases with $T_{IC,PBS}$, and such larger thickness favors the formation of thicker PEO crystal as the PEO component mainly crystallizes in the interlamellar region in these blends. It is also noteworthy that the decrease of $T_{m,PEO}$ with the increase of $T_{C,PEO}$ as shown in Figure 6 should not mean that the decrease of $T_{m,PEO}$ is due to the increase of $T_{C,PEO}$. Under the conditions studied here, $T_{m,PEO}$ is a function of $T_{IC,PBS}$ rather than $T_{C,PEO}$ to some extent.

5. Conclusion

The crystallization behavior of the PEO component in the PBS/PEO blends with middle PEO content (30−50 wt %) is significantly affected by the isothermal crystallization temperature of the PBS component $T_{IC,PBS}$. On the basis of the SAXS measurements and combined the results of our previous work, it is suggested that $T_{IC,PBS}$ controls the positional distribution of the PEO component after the crystallization of the PBS component. Higher $T_{IC,PBS}$ may favor the incorporation of the PEO component in the region between PBS lamellae while lower $T_{IC,PBS}$ may favor the exclusion of the PEO component from the interlamellar region. As a result, the PEO component in the PBS/PEO blends with middle PEO content only crystallizes at high supercooling if the PBS component crystallizes at high $T_{IC,PBS}$ and vice versa.

References and Notes

(1) (a) Arnal, M. L.; Matos, M. E.; Morales, R. A.; Santana, O. O.; Muller, A. J. *Macromol. Chem. Phys.* **1998**, *199*, 2275. (b) Frensch, H.; Jungnickel, B. J. *Colloid Polym. Sci.* **1989**, *267*, 16. (c) Frensch, H.; Harnischfeger, P. Jungnickel, B. J. Fractional Crystallization in Incompatible Polymer Blends. In *Multiphase Polymers: Blends and Ionomers*; Utracky, L. A., Weiss, R. A., Eds.; *ACS Symp. Ser.* **1989**, *395*, 101. (d) Frensch, H.; Jungnickel, B. J. *Plast. Rubber Compos. Process. Appl.* **1991**, *16*, 5. (e) Arnal, M. L.; Müller, A. J.; Maiti, P.; Hikosaka, M. *Macromol. Chem. Phys.* **2000**, *201*, 2493. (f) Arnal, M. L.; Müller, A. J. *Macromol. Chem. Phys.* **1999**, *200*, 2559. (g) Molinuevo, C. H.; Mendez, G. A.; Muller, A. J. *J. Appl. Polym. Sci.* **1998**, *70*, 1725. (h) Everaert, V.; Groeninckx, G.; Koch, M. H. J.; Reynaers, H. *Polymer* **2003**, *44*, 3491. (i) Kowaleski, T.; Ragosta, G.; Martuscelli, E.; Galeski, A. *J. Appl. Polym. Sci.* **1997**, *66*, 2047.

(2) (a) Xu, J.; Fairclough, J. P. A.; Mai, S.; Ryan, A. J.; Chaibundit, C. *Macromolecules* **2002**, *35*, 6937. (b) Loo Y. L.; Register, R. A.; Ryan, A. J. *Phys.* Rev. Lett. **2000**, *84*, 4120. (c) Segalman, R. A.; Hexemer, A.; Kramer, E. J. *Macromolecules* **2003**, *36*, 6831. (d) Schmalz, H.; Knoll, A.; Muller, A. J.; Abetz, V. *Macromolecules* **2002**, *35*, 10004. (e) Schipper, F. J. M.; Floudas, G.; Pispas, S.; Hadjichristidis, N.; Pakula, T. *Macromolecules* **2002**, *35*, 8860. (f) Opitz, R.; Lambreva, D. M.; de Jeu, W. H. *Macromolecules* **2002**, *35*, 6930. (g) Zhu, L.; Huang, P.; Chen, W. Y.; Ge, Q.; Quirk, R. P.; Cheng, S. Z. D.; Thomas, E. L.; Lotz, B.; Hsiao, B. S.; Yeh, F.; Liu, L. *Macromolecules* **2002**, *35*, 3553.

(3) (a) Schonherr, H.; Frank, C. W. *Macromolecules* **2003**, *36*, 1188. (b) Schonherr, H.; Frank, C. W. *Macromolecules* **2003**, *36*, 1199. (c) Reiter, G. *J. Polym. Sci., Part B: Polym. Phys.* **2003**, *41*, 1869.

(4) Cormia, R. L.; Price, F. P.; Turnbull, D. *J. Chem. Phys.* **1962**, *37*, 1333.

(5) Taden, A.; Landfester, K. *Macromolecules* **2003**, *36*, 4037.

(6) He, Y.; Zhu, B.; Kai, W.; Inoue, Y. *Macromolecules* **2004**, *37*, 3337.

(7) Huot, P. P.; Cebe, P.; Cape1, M. *Macromolecules* **1993**, *26*, 4215.

(8) Bristow, J. F.; Kalika, D. S. *Polymer* **1997**, *38*, 287.

(9) Chen, H. L.; Wang, S. F. *Polymer* **2000**, *41*, 5157.

(10) Qiu, Z.; Ikehara, T.; Nishi, T. *Polymer* **2003**, *44*, 2799.

(11) Campbell, C.; Viras, K.; Richardson, M. J.; Masters, A. J.; Booth, C. *Makromol. Chem.* **1993**, *194*, 799.

(12) Yang, Z.; Yu, G. E.; Cooke, J.; Ali-Adib, Z.; Viras, K.; Matsuura, H.; Ryan, A. J.; Booth, C. *J. Chem. Soc., Faraday Trans.* **1996**, *92*, 3173.

(13) Xu, J.; Fairclough, J. P. A.; Mai, S.; Ryan, A. J.; Chaibundit, C. *Macromolecules* **2002**, *35*, 6937.

(14) Cooke, J.; Viras, K.; Yu, G. E.; Sun, T.; Yonemitsu, T.; Ryan, A. J.; Price, C.; Booth, C. *Macromolecules* **1998**, *31*, 3030.

(15) Glatter, O.; Kratky, O. *Small-Angle X-ray Scattering;* Academic Press: London, 1982.

(16) Kruger, K. N.; Zachmann, H. G. *Macromolecules* **1993**, *26*, 5202.

(17) Ihn, K. J.; Yoo, E. S.; Im, S. S. *Macromolecules* **1995**, *28*, 2460.

(18) Ichikawa, Y.; Kondo, H.; Igarashi, Y.; Noguchi, K.; Okuyama, K.; Washiyama, J. *Polymer* **2000**, *41*, 4719.

(19) Yoo, E. S.; Im, S. S. *J. Envirom. Polym. Degrad.* **1997**, *7*, 19.

(20) Miyata, T.; Masuko, T. *Polymer* **1998**, *39*, 1399.

(21) Wunderlich, B. *Macromolecular Physics*; Academic Press: New York, 1980; Vol. 3. p 67.

(22) Brandrup, J., Immergut, E. H., Eds.; *Polymer Handbook*, 3rd ed.; Wiley: New York, 1989.

(23) Avella, M.; Martuscelli, E.; Raimo, M. *Polymer* **1993**, *34*, 3234.

(24) Kit, K. M.; Schultz, J. M. *J. Polym. Sci., Part B: Polym. Phys.* **1998**, *36*, 873.

(25) Kit, K. M.; Schultz, J. M. *Macromolecules* **2002**, *35*, 9819.

(26) Keith, H. D.; Padden, F. J. *J. Appl. Phys.* **1963**, *34*, 2409.

(27) Gan, Z.; Abe, H.; Kurokawa, H.; Doi, Y. *Biomacromolecules* **2001**, *2*, 605.

(28) Jina, H. J.; Leeb, B. Y.; Kimb, M. N.; Yoon, J. S. *Eur. Polym. J.* **2000**, *36*, 2693.

MA049482F